

# Quasinormal modes of regular black holes with sub-Planckian curvature and Minkowskian core

Chen Tang<sup>1,\*</sup> Yi Ling<sup>2,3,1,†</sup> Qing-Quan Jiang<sup>1,‡</sup> and Guo-Ping Li<sup>1,§</sup>

<sup>1</sup> *School of Physics and Astronomy,*

*China West Normal University, Nanchong 637002, China*

<sup>2</sup> *Institute of High Energy Physics,*

*Chinese Academy of Sciences, Beijing 100049, China*

<sup>3</sup> *School of Physics, University of Chinese Academy of Sciences, Beijing 100049, China*

## Abstract

We investigate the perturbation of the scalar field as well as the electromagnetic field over a sort of regular black holes which are characterized by the sub-Planckian curvature and the Minkowskian core. Specifically, we compute the quasinormal modes(QNMs) by employing the pseudo-spectral method. The outburst of overtones is manifestly observed in the QNMs of these regular black holes, which can be attributed to the deviation of the Schwarzschild black hole by quantum effects of gravity. Furthermore, the QNMs under the perturbation of electromagnetic field exhibit smaller real and imaginary parts than those under scalar field perturbation. By comparing the QNMs of the regular black hole featured by Minkowskian core with those of Bardeen black hole featured by de Sitter core, we find they may be an effective tool to distinguish these BHs.

---

\*Electronic address: ctangphys@stu.cwnu.edu.cn

†Electronic address: liny@ihep.ac.cn(Corresponding author)

‡Electronic address: qqjiangphys@yeah.net(Corresponding author)

§Electronic address: gpliphys@yeah.net(Corresponding author)

## I. INTRODUCTION

The quasinormal modes (QNMs) as the intrinsic feature of a black hole have been playing a vital role in black hole physics (For comprehensive review on QNMs, we refer to recent Ref.[1–4]). By considering the perturbations surrounding a black hole and computing the QNMs, one may acquire the parameter information of a black hole such as the mass and spin[5–7]. Furthermore, one may diagnose the stability of a black hole by the feature of its QNMs[8–18]. More importantly, QNMs is an important tool for analyzing and interpreting gravitational wave signals generated by the merger of binary black holes[19–26]. In addition, one can use QNMs to investigate the internal structure and dynamical behavior of extremal compact objects such as neutron stars [1, 27–29]. In particular, since the first signal of gravitational waves was successfully detected by LIGO in 2015 [30, 31] and the first image of the black hole at the center of the M87 galaxy was captured by EHT in 2019 [32], the QNMs have been becoming the powerful tool for linking the theory on black holes to the data of observation. The analysis on QNMs is of great significance for exploring the nature of black holes and for testing various theories on gravity by astronomical observation.

Recently, the QNMs of regular black holes have been extensively investigated with the purpose of revealing the internal structure of black holes and capturing the possible signals due to the quantum effects of gravity [33–48]. Regular black holes are those without singularity at the center of the black hole [49–52], thus not suffering from the singularity problem as those black holes in standard general relativity [53, 54]. Originally, regular black holes are proposed by purely phenomenological consideration, with the assumption that the singularity would be removed by the quantum effect of gravity[49–52, 55–59]. Later, people find that they can also be constructed as the solutions to Einstein equations with exotic matter which locally violates the energy conditions[60–64], or to the effective Einstein equations which take the quantum correction of gravity into account[65–68] (For recent review on regular black holes, we refer to Refs.[69, 70]). By perturbative analysis, it is quite interesting to notice that the QNMs of regular black holes exhibit some distinct behavior from those of black holes with singularity, thus in principle one could diagnose if the observed astrophysical black holes contain the singularity inside by examining their QNMs in future. For instance, the outburst of overtones is manifestly observed in the QNMs of regular black holes, which might be ascribed to the quantum effects of gravity [71–83]. Recently, a new

sort of regular black holes with an exponentially suppressing Newton potential are proposed in [84], which is characterized by the sub-Planckian curvature and the Minkowskian core. Sequentially, the observational feature of these regular black holes are investigated in [85–89]. Specially, the QNMs of a specific regular black hole which has the same asymptotic behavior with Hayward black hole at infinity is investigated in [48]. In this paper we intend to push this approach forward by considering the QNMs of a regular black hole which has the same asymptotic behavior with Bardeen black hole. The QNMs of both the scalar field and the electromagnetic field will be investigated. More importantly, we will compare the QNMs of this sort of regular black holes with different deviation parameters. It is expected that the current work will provide more information about the QNMs of this sort of regular black holes and then applicable to distinguish regular black holes from singular black holes by the observation in near future.

The paper is organized as follows. In Section II, we briefly review the regular black holes with Minkowskian core and sub-Planckian curvature originally proposed in [84]. Then in Section III, we investigate the QNMs of a typical regular black hole with specific parameters under scalar and electromagnetic field perturbations in detail. The QNMs of the regular black hole featured by Minkowskian core with those of Bardeen black hole featured by de Sitter core is compared in Section IV. In Section V, we compare the QNMs of regular black holes with different parameters under scalar field perturbations. We summarize our results and discuss the possible progress in future in Section VI.

## II. REGULAR BLACK HOLES WITH MINKOWSKIAN CORE AND SUB-PLANCKIAN CURVATURE

In this section, we briefly review the spherically symmetric regular black hole with sub-Planckian curvature originally proposed in [84]. This sort of regular black holes is characterized by an asymptotically Minkowski core as well as an exponentially suppressing gravity potential. Specifically, their metric takes the following form

$$ds^2 = -f(r)dt^2 + \frac{1}{f(r)}dr^2 + r^2 (d\theta^2 + \sin^2\theta d\phi^2), \quad (1)$$

where the function  $f(r)$  is given by

$$f(r) = 1 + 2\psi(r) = 1 - \frac{2M}{r} e^{-\frac{\alpha_0 M^x}{r^c}}, \quad (2)$$

where  $M$  is the mass of black hole and the parameters  $x$ ,  $c$ ,  $\alpha_0$  are all the dimensionless parameters<sup>1</sup>. Importantly,  $\alpha_0$  indicates the degree of deviation from the Newtonian potential and characterizes the corrections due to quantum gravity effects[55, 56]. Obviously, when  $\alpha_0 = 0$ , the potential reduces to the standard Newtonian potential and this regular BH goes back to an ordinary Schwarzschild BH. In addition, to preserve the spacetime curvature to be sub-Planckian, the parameters should satisfy the conditions  $c \geq x \geq c/3$  and  $c \geq 2$  [84]. Previously, the QNMs of the scalar field over regular black hole with  $x = 1$  and  $c = 3$  was studied in [48], with a comparison with the QNMs of Hayward black hole. In this paper, we will extend the above analysis to the QNMs of both the scalar field and the electromagnetic field over the regular black hole with  $x = 2/3$  and  $c = 2$  at first, which has the same asymptotic behavior at infinity as the Bardeen BH. Moreover, we will compare the QNMs of this sort of regular black holes with general parameters  $x$  and  $c$  under the above sub-Planckian conditions. For the metric with the function in (2), the event horizon can be obtained by solving the equation  $f(r_h) = 0$ , and  $r_h$  is the location of the event horizon. Then, it is straightforward to derive the Hawking temperature as

$$T = \frac{f'(r_h)}{4\pi} = \frac{\psi'(r_h)}{2\pi}. \quad (3)$$

By substituting Eq.(2) into Eq.(3), the specific form of Hawking temperature can be expressed as

$$T = \frac{e^{-\frac{M^{2/3}\alpha_0}{r_h^2}} M (r_h^2 - 2M^{2/3}\alpha_0)}{2\pi r_h^4}. \quad (4)$$

Here, the Hawking temperature should be greater than zero, implying that the deviation parameter  $\alpha_0$  is constrained as

$$\alpha_0 \leq \frac{2M^{4/3}}{e}. \quad (5)$$

In FIG. 1, we plot the Hawking temperature as a function of the deviation parameter  $\alpha_0$  with  $M = 1$ . It can be seen that the temperature  $T$  decreases as  $\alpha_0$  increases until it drops to zero at  $\alpha_0 = 2/e$ . Finally, we remark that the regular black hole with  $x = 2/3$  and  $c = 2$  has the same asymptotic behavior at infinity as the Bardeen black hole. At large scales

---

<sup>1</sup> We have set  $8\pi G = l_p^2 = 1$  throughout this paper for convenience. It means if one intends to recover the dimension of the potential, it should become as  $\psi(r) = -\frac{MG}{r} e^{-\frac{\alpha_0(MG)^{x_1} l_p^{c-x}}{r^c}}$ .

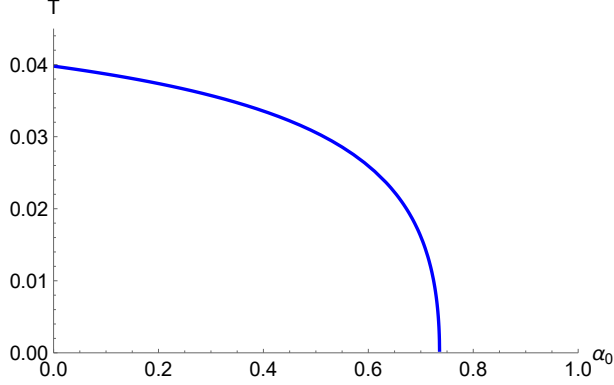


FIG. 1: The Hawking temperature as a function of  $\alpha_0$ , where  $r_h = 1$  and  $M = 1$ .

where  $r \gg \sqrt{\alpha_0}M^{1/3}$ , the function  $f(r)$  can be expanded as the following form

$$f(r) = 1 + 2\psi(r) = 1 - \frac{2M}{r}e^{-\alpha_0 M^{2/3}/r^2} \cong 1 - \frac{2M}{r}\left(1 - \frac{\alpha_0 M^{2/3}}{r^2} + \dots\right). \quad (6)$$

On the other hand, the function  $\psi$  of the Bardeen black hole has the form

$$\psi(r) = -\frac{Mr^2}{\left(\frac{2}{3}\alpha_0 M^{2/3} + r^2\right)^{3/2}}. \quad (7)$$

So, at large scales the function  $f(r)$  asymptotically behaves as

$$f(r) = 1 + 2\psi(r) = 1 - \frac{2Mr^2}{\left(\frac{2}{3}\alpha_0 M^{2/3} + r^2\right)^{3/2}} \cong 1 - \frac{2M}{r}\left(1 - \frac{\alpha_0 M^{2/3}}{r^2} + \dots\right), \quad (8)$$

which is the same as the regular black hole with  $x = 2/3$  and  $c = 2$ . Nevertheless, we point out that these two black holes exhibit distinct behavior at the center of the black hole. As  $r \rightarrow 0$ , the regular black hole with  $x = 2/3$  and  $c = 2$  has a Minkowskian core while Bardeen black hole has a de-Sitter core. In this paper we are concerned with the behavior of QNMs in these two regular black holes when the parameter  $\alpha_0$  takes the same value.

### III. QUASINORMAL MODES OF THE REGULAR BLACK HOLE WITH $x = 2/3$ AND $c = 2$

In this section, we study the QNMs of the regular black hole with  $x = 2/3$  and  $c = 2$  under the perturbation of the scalar and electromagnetic field, respectively. In general, the asymptotic behavior of the QNM close to the boundary should satisfy

$$\Psi \sim e^{-i\omega(t+r_*)} \quad r_* \rightarrow +\infty, \quad (9a)$$

$$\Psi \sim e^{-i\omega(t-r_*)} \quad r_* \rightarrow -\infty, \quad (9b)$$

where  $r_*$  is the ordinary radial tortoise coordinate. This indicates that the QNMs at the event horizon are purely ingoing waves, while at infinity are purely outgoing waves. In this section, we consider the perturbation of scalar field and electromagnetic field, which are described by the Klein-Gordon equation and the Maxwell equations, respectively

$$\frac{1}{\sqrt{-g}}(g^{\mu\nu}\sqrt{-g}\partial_\mu\Phi)_{,\nu} = 0, \quad (10a)$$

$$\frac{1}{\sqrt{-g}}(g^{\alpha\mu}g^{\sigma\nu}\sqrt{-g}F_{\alpha\sigma})_{,\nu} = 0, \quad (10b)$$

where  $g^{\mu\nu}$  is the contravariant form of the metric, and  $g$  is its determinant. By virtue of the spherical symmetry of the background, one can separate variables and decompose the wave function into the form of spherical harmonic functions. For instance, for the scalar field, it can be decomposed as

$$\Phi(t, r, \theta, \phi) = \sum_{l,m} Y_{l,m}(\theta, \phi) \frac{\Psi_{l,m}(t, r)}{r}, \quad (11)$$

where  $Y_{l,m}(\theta, \phi)$  denotes the spherical harmonic function, with the symbols  $l$  and  $m$  representing the angular quantum number and magnetic quantum number, respectively. The similar decomposition can be performed for the Maxwell field and we refer to [82] for details. Substituting Eq.(11) into the perturbation Eq.(10), and further performing the tortoise coordinate transformation ( $dr_*/dr = 1/f(r)$ ), one changes both the Klein-Gordon equation and Maxwell equation into a Schrödinger-like form, which is

$$\frac{\partial^2\Psi}{\partial r_*^2} + (\omega^2 - V_{eff})\Psi = 0. \quad (12)$$

We are concerned with the solution of the wave function as the values of  $l$  and  $m$  are given for the spherical harmonics, thus for convenience, the lower indices  $l$  and  $m$  are omitted in the notation of the wave function in the following. The effective potential in the Schrödinger-like equation is

$$V_s(r) = f(r) \left( \frac{l(l+1)}{r^2} + (1-s)\frac{f'(r)}{r} \right). \quad (13)$$

When the spin  $s = 0$ , it corresponds to scalar perturbations; while for  $s = 1$ , it corresponds to electromagnetic perturbations.

A lot of methods have been presented in literature for one to compute the QNMs, including the Wentzel–Kramers–Brillouin (WKB) method, the pseudo-spectral(ps) method, the continued fraction method [90], Horowitz-Hubeny method [8], asymptotic iteration method [91] and the matrix method [92, 93]. In this paper we will employ pseudo-spectral method to

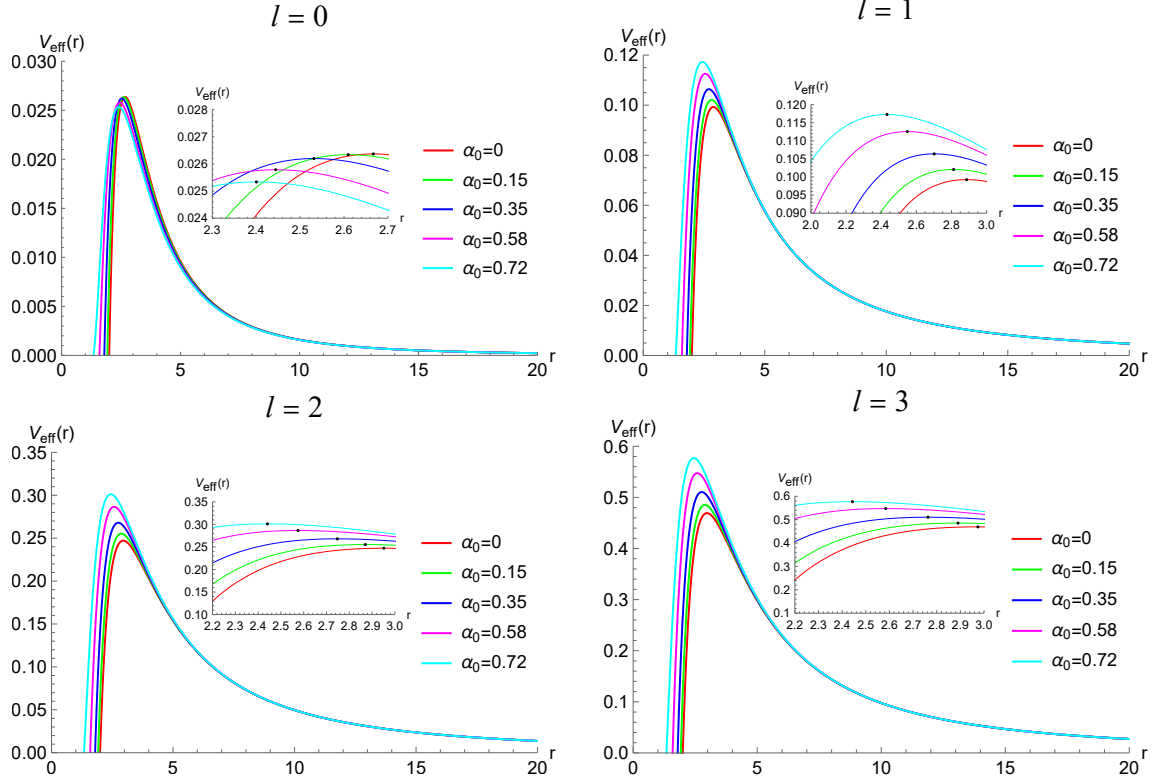


FIG. 2: The effective potential  $V_{\text{eff}}(r)$  of the scalar field with different deviation parameters  $\alpha_0$ . The black dot represents the maximum value of the  $V_{\text{eff}}(r)$ .

numerically investigate the QNMs of regular black holes <sup>2</sup>, while the details of the pseudo-spectral method can be referred to Appendix A.

### A. The QNMs under the perturbation of a scalar field

Obviously, the specific form of the effective potential plays a key role in determining the QNMs of the perturbations. In FIG. 2, we plot the effective potential  $V_{\text{eff}}(r)$  of the scalar field with different deviation parameters  $\alpha_0$ . It shows that the effective potential is always positive, indicating that the spacetime of this regular BH is stable under the scalar perturbations. Furthermore, the effective potential increases with the increase of  $l$ . Also, it is interesting to notice that the maximal value of the potential  $V_{\text{eff}}$  decreases as  $\alpha_0$  increases

<sup>2</sup> In fact, we have also employed the WKB method to study the the QNMs of regular black holes (1), and obtained the similar conclusion with [48], i.e., the WKB method is not quite suitable for computing highly damped QNMs. This part of the content is not the focus of our article.

for  $l = 0$ ; while for  $l = 1, 2, 3$ , its maximal value increases with  $\alpha_0$ . We remark that this special behavior of the effective potential at  $l = 0$  might be responsible for the spiral behavior of QNMs that appears in the first few overtones, as illustrated in the next context.

Now we present the numerical results for the QNMs of regular black hole under the perturbation of scalar field, which are obtained with the pseudo-spectral method. In Tables (I), (II) and (III), we list the frequency of the QNMs for different overtone numbers  $n$  and deviation parameters  $\alpha_0$ .

n	$\alpha_0 = 0$	$\alpha_0 = 0.3$	$\alpha_0 = 0.5$	$\alpha_0 = 2/e$
0	0.110455-0.104896i	0.115834-0.100752i	0.119115-0.095696i	0.116896-0.088312i
1	0.086117-0.348053i	0.093067-0.330182i	0.090531-0.309631i	0.074856-0.309121i
2	0.075776-0.601067i	0.080399-0.569011i	0.052095-0.537955i	0.055515-0.553466i

TABLE I: The frequency of QNMs under scalar perturbations for  $l = 0$

n	$\alpha_0 = 0$	$\alpha_0 = 0.3$	$\alpha_0 = 0.5$	$\alpha_0 = 2/e$
0	0.292936-0.09766i	0.304502-0.094405i	0.313652-0.090570i	0.325102-0.082546i
1	0.264449-0.306257i	0.280096-0.293848i	0.290682-0.279744i	0.294583-0.255512i
2	0.229539-0.540133i	0.248559-0.513917i	0.256659-0.485222i	0.242126-0.453212i
3	0.203258-0.788298i	0.222508-0.746671i	0.219932-0.703117i	0.190160-0.681290i
4	0.185109-1.040760i	0.202301-0.983759i	0.177099-0.930025i	0.155153-0.931619i
5	0.172080-1.294130i	0.185453-1.221950i	0.136329-1.195380i	0.128669-1.176260i

TABLE II: The frequency of QNMs under scalar perturbations for  $l = 1$ .

In each table the angular momentum  $l$  is fixed as  $l = 0$ ,  $l = 1$  and  $l = 2$ , respectively. Firstly, it shows that the imaginary part of all QNM frequencies is always negative, indicating that the regular BH is stable under the scalar perturbations. Secondly, we are concerned with the effects of the overtone number  $n$  and quantum number  $l$  on the QNMs. In each table with fixed  $l$ , we notice that with the increase of the overtone number  $n$ , the real part of QNMs decreases and the imaginary part increases, indicating that the QNMs exhibit weaker oscillations and faster decay with  $n$ , which is similar to that of ordinary black holes with

$n$	$\alpha_0 = 0$	$\alpha_0 = 0.3$	$\alpha_0 = 0.5$	$\alpha_0 = 2/e$
0	0.483644-0.096759i	0.502162-0.093662i	0.517272-0.090012i	0.538533-0.081991i
1	0.463851-0.295604i	0.485334-0.285272i	0.501871-0.273277i	0.519576-0.248721i
2	0.430544-0.508558i	0.456643-0.488169i	0.474525-0.465111i	0.482746-0.424192i
3	0.393863-0.738097i	0.423946-0.704539i	0.440578-0.667589i	0.431833-0.615047i
4	0.361299-0.979922i	0.393356-0.931434i	0.404192-0.879340i	0.375024-0.825865i
5	0.334900-1.228410i	0.366972-1.164490i	0.366463-1.098090i	0.322525-1.054220i

TABLE III: The frequency of QNMs under scalar perturbations for  $l = 2$ .

singularity. On the other hand, if we fix  $n$  and  $\alpha_0$  but change  $l$ , then we notice that the real part of the QNM frequency becomes larger as  $l$  increases. The reason is that as  $l$  increases, the effective potential becomes larger as well, as illustrated in FIG. 2. Thus it requires that the vibration frequency of the wave becomes larger such that the QNMs can escape from the potential and transmit to infinity. However, the imaginary part of the frequency does not change much as  $l$  increases, implying that the attenuation rate of the QNM is majorly determined by the parameter  $n$  rather than  $l$ . Next, we focus on the effect of the deviation parameter  $\alpha_0$ , which is the major part that we are concerned with. For  $l = 0$  in Table (I), we notice that the real part increases initially and then decreases with the increase of the parameter  $\alpha_0$ , while for  $l = 1$  and  $l = 2$ , it becomes monotonously increasing with  $\alpha_0$  for smaller  $n$ , but again exhibits the similar behavior as  $l = 0$  for larger  $n$ . Similarly, we find that the monotonous behavior of the imaginary part stops with the increase of the overtone number  $n$ .

To reveal the behavior of the QNMs with the variation of  $\alpha_0$  more transparently, we intend to plot the trajectory of the QNMs on the plane of the complex frequency. For each specified  $n$  and  $l$ , we compute the frequency of the QNMs as the deviation parameter  $\alpha_0$  runs from zero to  $2/e$ , and then plot a trajectory on the plane of the complex frequency, as illustrated in FIG. 3 to FIG. 5, where  $l$  and  $n$  are specified as various values.

The feature of the QNMs demonstrated in these figures can be summarized as follows,

1. Firstly, once  $\alpha_0$  and  $l$  are fixed, the real part of the QNM frequency decreases with the increase of the overtone number  $n$ , while the imaginary part increases, which directly leads to a faster decay of the QNMs.

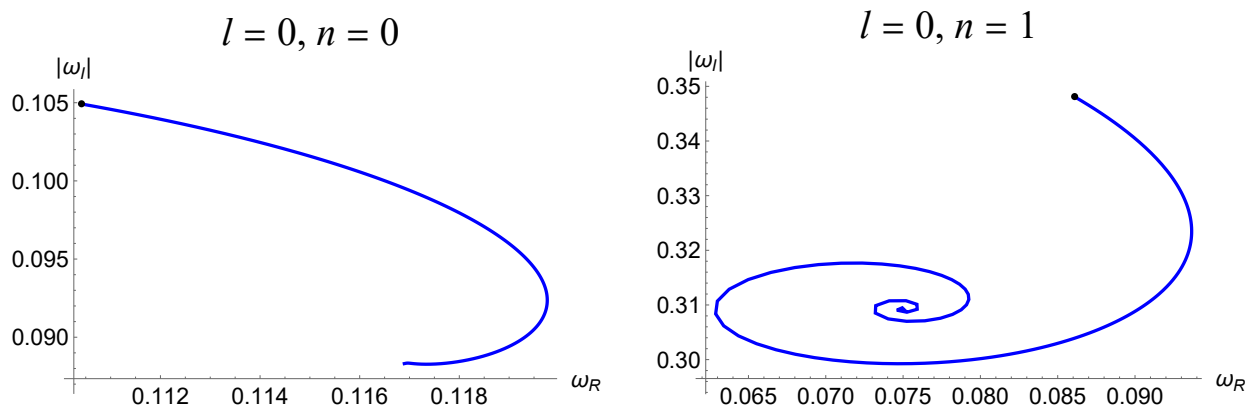


FIG. 3: The trajectory of the QNMs with the variation of  $\alpha_0$  on the frequency plane with  $l = 0$ , where  $\omega_R$  is the real part and  $|\omega_I|$  is the magnitude of the imaginary part. The black dots denote the QNM of Schwarzschild black hole, which is same in the following figures.

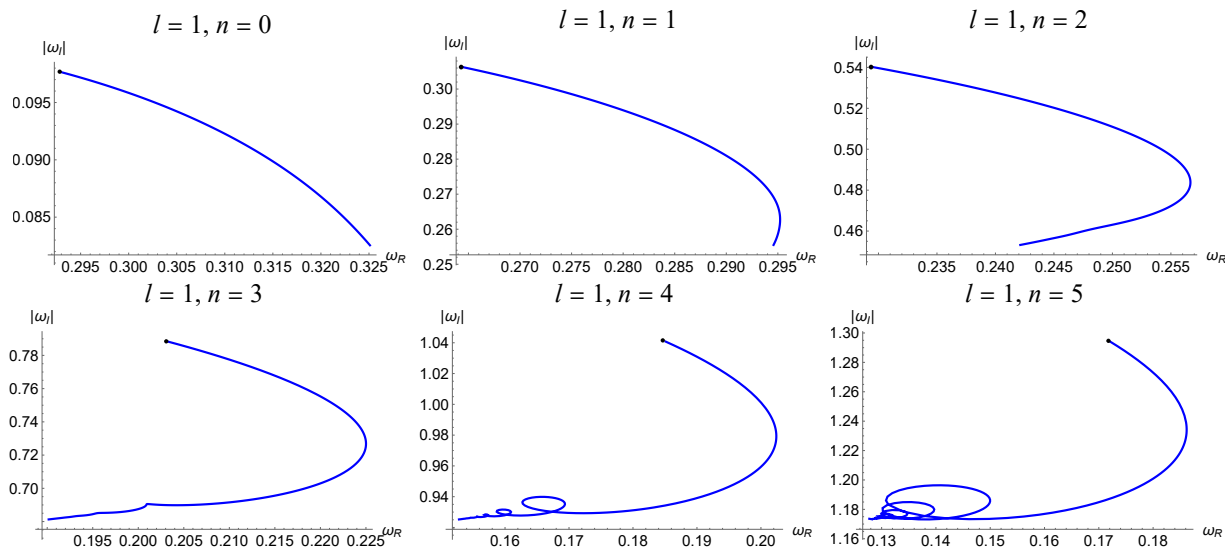


FIG. 4: The trajectory of the QNMs with the variation of  $\alpha_0$  on the frequency plane with  $l = 1$  under scalar field perturbation.

2. When  $\alpha_0$  and  $n$  are fixed, the increase of the angular quantum number  $l$  leads to the increase of the real part of the frequency, while the imaginary part remains almost unchanged. This is because the effective potential increases with  $l$ , and it requires that the wave acquires greater energy to propagate to infinity.

3. With the running of  $\alpha_0$ , the QNMs frequency intend to exhibit a non-monotonic behavior and spiral behavior. When  $l$  is fixed at  $l = 0, 1$ , as the overtone number  $n$  increases,

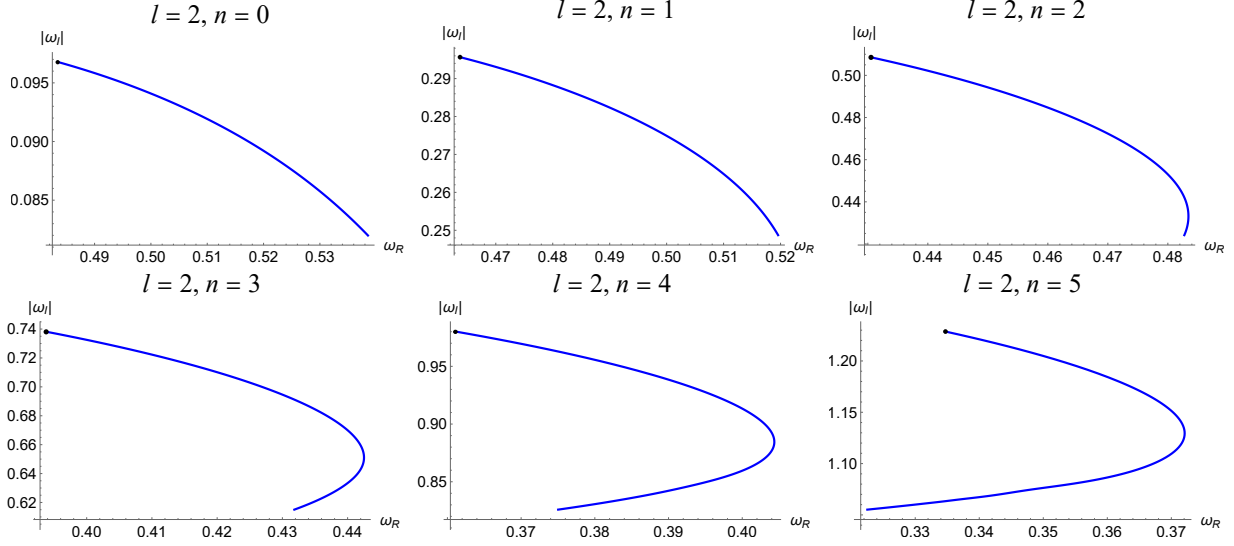


FIG. 5: The trajectory of the QNMs with the variation of  $\alpha_0$  on the frequency plane with  $l = 2$  under scalar field perturbation.

the non-monotonic behavior becomes more evident and may evolve into a trajectory with a spiral behavior, for instance in figures for  $(l = 0, n = 1)$ ,  $(l = 1, n = 4)$  and  $(l = 1, n = 5)$ . However, an increase in the angular momentum quantum number  $l$  seems to suppress this non-monotonic behavior. For instance, when  $l = 2$ , the non-monotonic behavior is not evident until  $n > 2$  and the spiral behavior of the trajectory does not appear in all the figures with  $n \leq 5$ .

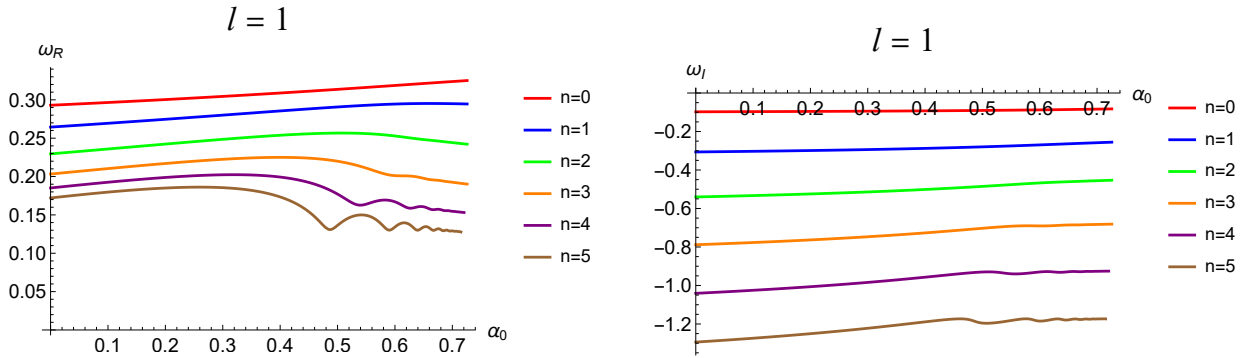


FIG. 6: The real and imaginary parts of QNMs as the function of  $\alpha_0$  with  $l = 1$  under scalar field perturbation.

To manifestly demonstrate the change of the QNMs frequency with the parameter  $\alpha_0$ , we may directly plot the real part and the imaginary part of the frequency as the function of

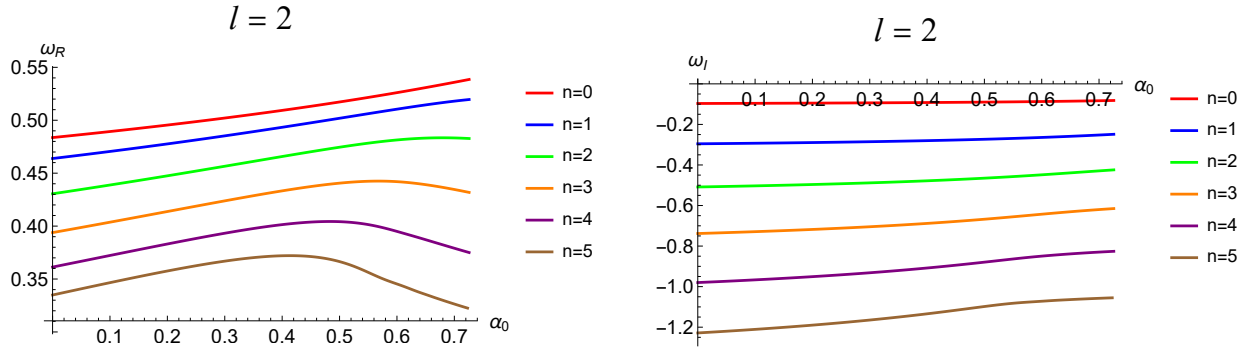


FIG. 7: The real and imaginary parts of QNMs as the function of  $\alpha_0$  with  $l = 2$  under scalar field perturbation.

$\alpha_0$  separately, as illustrated in FIG. 6 for  $l = 1$  and FIG. 7 for  $l = 2$ . It is evident that when  $l = 1$  and the value of  $n$  reaches to 4 and 5, the real part exhibits significant oscillatory behavior, known as the outburst phenomenon. The imaginary part also exhibits the outburst phenomenon in the cases of  $n = 4$  and  $n = 5$ . Furthermore, the higher the overtone number  $n$ , the more pronounced the oscillatory behavior becomes in both the real and imaginary parts. These oscillations in the real and imaginary parts contribute to the spiral behavior observed in the previous figures. However, when  $l = 2$ , the oscillatory behavior becomes weak and disappearing, as shown in FIG. 7. In addition, the real part only exhibits the non-monotonic behavior for  $n = 3$ ,  $n = 4$  and  $n = 5$ , while the imaginary part remains almost unchanged. It is expected to confirm whether a higher overtone number  $n$  would cause the non-monotonic behavior and further evolve into oscillatory behavior in future.

### B. The QNMs under the perturbation of electromagnetic field

In this subsection we continue to investigate the response of the regular black hole under electromagnetic field perturbations. In parallel, the QNMs of the regular black hole under electromagnetic field perturbations can be computed for different values of  $l, n, \alpha_0$ , which have been summarized in Tables (IV), (V) and FIG. 8, 9, 10 and 11.

We notice that the QNMs under electromagnetic field perturbation exhibit the similar behavior as those under the scalar field perturbation. In particular, it can be seen from FIG. 8 and FIG. 9 that for  $l = 1$ , the spiral behavior can be obviously observed with the increase of  $n$ , while for  $l = 2$ , the behavior disappears. Qualitatively this observed phenomenon is

$n$	$\alpha_0 = 0$	$\alpha_0 = 0.3$	$\alpha_0 = 0.5$	$\alpha_0 = 2/e$
0	0.248263-0.092488i	0.261020-0.089823i	0.271566-0.086200i	0.285600-0.077192i
1	0.214515-0.293668i	0.232596-0.282407i	0.246087-0.268233i	0.252756-0.239495i
2	0.174774-0.525188i	0.197380-0.499535i	0.210289-0.469126i	0.195035-0.428313i
3	0.146176-0.771909i	0.169757-0.730175i	0.174524-0.681999i	0.137729-0.650895i
4	0.126548-1.022530i	0.148845-0.964811i	0.136150-0.900198i	0.096489-0.890878i
5	0.112103-1.273890i	0.131601-1.200420i	0.079902-1.127980i	0.068540-1.134290i

TABLE IV: The frequency of QNMs under electromagnetic perturbations for  $l = 1$ .

$n$	$\alpha_0 = 0$	$\alpha_0 = 0.3$	$\alpha_0 = 0.5$	$\alpha_0 = 2/e$
0	0.457596-0.095004i	0.476647-0.092046i	0.492386-0.088424i	0.514945-0.080055i
1	0.436542-0.290710i	0.458901-0.280724i	0.476425-0.268720i	0.495597-0.242907i
2	0.401187-0.501587i	0.428766-0.481513i	0.448256-0.458131i	0.457868-0.414559i
3	0.362595-0.730199i	0.394796-0.696651i	0.413739-0.658717i	0.405478-0.601951i
4	0.328737-0.971609i	0.363491-0.922730i	0.377384-0.868702i	0.346929-0.810019i
5	0.301493-1.21971i	0.336867-1.154990i	0.340336-1.085250i	0.293947-1.037730i

TABLE V: The frequency of QNMs under electromagnetic perturbations for  $l = 2$ .

similar to that in the case of the scalar field perturbation. Furthermore, the occurrence of the spiral behavior on the plane of the complex frequency can be reflected by the oscillatory behavior of the real and imaginary parts of the QNMs as the function of the deviation parameter  $\alpha_0$ , as illustrated in FIG. 10 and 11.

In addition, in comparison with the QNMs under the scalar field perturbation, we find that the QNMs with the same parameters under electromagnetic field perturbation have smaller real and imaginary parts. This suggests that the QNMs under electromagnetic field perturbation have a lower oscillation frequency, as well as a weaker attenuation.

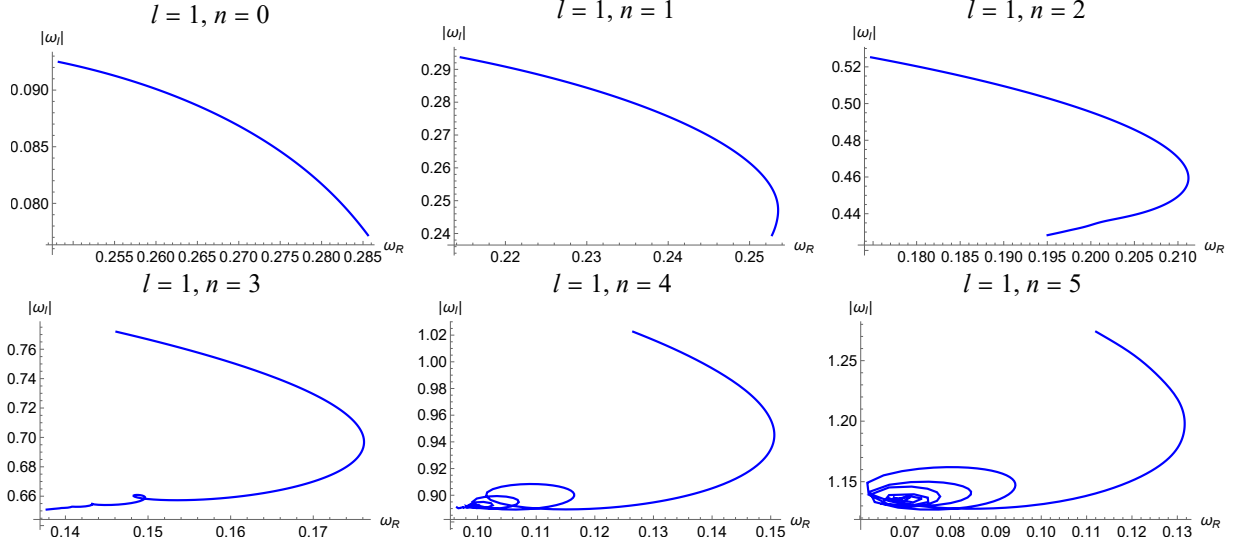


FIG. 8: The trajectory of the QNMs with the variation of  $\alpha_0$  on the frequency plane with  $l = 1$  under electromagnetic field perturbation

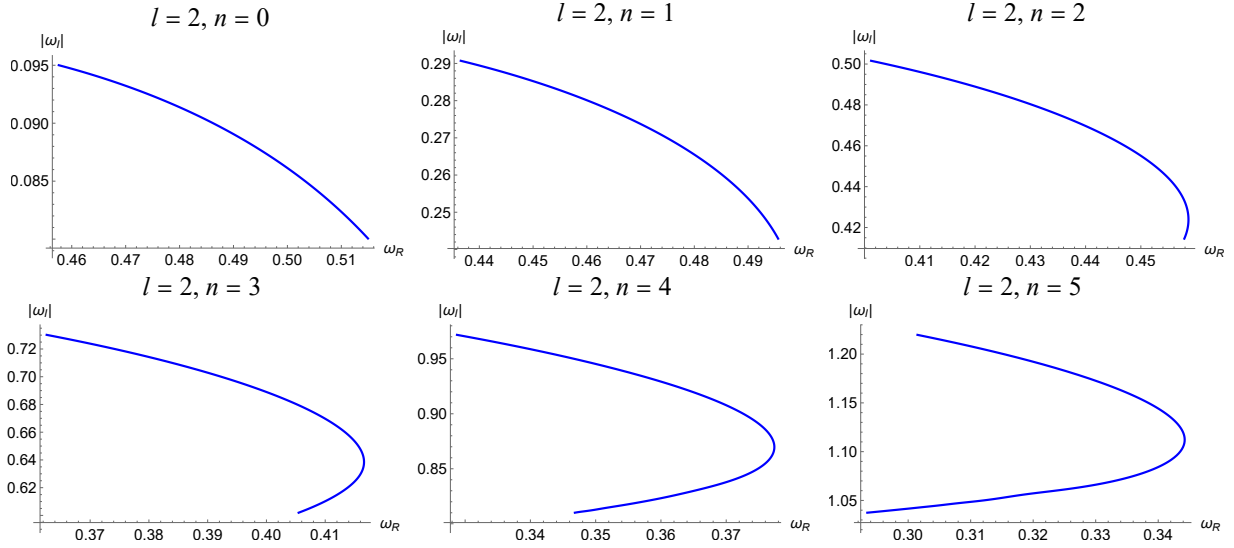


FIG. 9: The trajectory of the QNMs with the variation of  $\alpha_0$  on the frequency plane with  $l = 2$  under electromagnetic field perturbation.

#### IV. THE COMPARISON OF THE QNMS BETWEEN THIS REGULAR BLACK HOLE AND BARDEEN BLACK HOLE

As we mentioned in the previous section, the regular black hole with  $(x = 2/3, c = 2)$  has the same asymptotic behavior at infinity as the Bardeen black hole. The difference lies

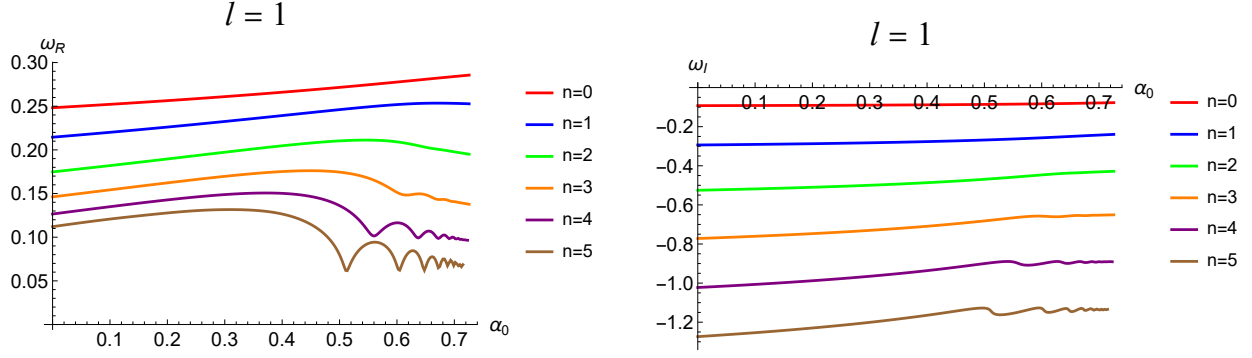


FIG. 10: The real and imaginary parts of QNMs as the function of  $\alpha_0$  with  $l = 1$  under electromagnetic field perturbation.

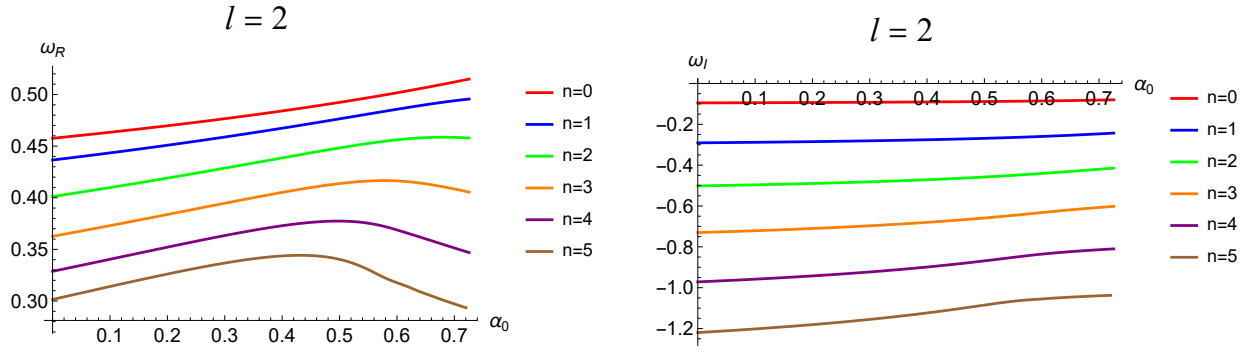


FIG. 11: The real and imaginary parts of QNMs as the function of  $\alpha_0$  with  $l = 2$  under electromagnetic field perturbation.

on the center of the black hole, as the former has a Minkowskian core while the latter has a de-Sitter core. It is quite interesting to compare the QNM behavior of these two regular black holes, that is what we intend to investigate in this section. Previously the QNMs of Bardeen black hole have been investigated in [94–99]. Here, we present the numerical results with the PS method, with a focus to compare its behavior with that of the regular black hole with  $(x = 2/3, c = 2)$ .

We investigate the QNMs of Bardeen black hole and define the discrepancy of the QNM frequency between Bardeen black hole and the regular black hole with  $(x = 2/3, c = 2)$  as

$$\Delta = \left| \frac{\omega_{Regular} - \omega_{Bardeen}}{\omega_{Regular}} \right| \times 100\%. \quad (14)$$

Table (VI) lists the QNMs of Bardeen BHs and the regular BH with  $(x = 2/3, c = 2)$  under the scalar field perturbation, while Table (VII) lists the QNMs under the electromag-

netic field perturbation.

$\alpha_0$	$n$	$\omega_{Regular}$	$\omega_{Bardeen}$	$\Delta$
0.15	0	0.298396-0.096297i	0.298395-0.096298i	$4.5 \times 10^{-4}\%$
	1	0.271993-0.300992i	0.271994-0.300997i	0.0013%
	2	0.239121-0.528880i	0.239127-0.528891i	0.0022%
	3	0.213779-0.770343i	0.213795-0.770359i	0.0028%
	4	0.195902-1.016091i	0.195933-1.016112i	0.0036%
	5	0.182764-1.262781i	0.182814-1.262811i	0.0046%
0.58	0	0.317685-0.088317i	0.317789-0.088508i	0.066%
	1	0.293929-0.271799i	0.294912-0.272364i	0.28%
	2	0.254437-0.470637i	0.258373-0.470546i	0.74%
	3	0.203826-0.689841i	0.213611-0.681019i	1.84%
	4	0.169328-0.935988i	0.152653-0.910328i	3.21%
	5	0.135243-1.173540i	0.114004-1.176200i	1.81%

TABLE VI: A comparison of the QNMs under scalar field perturbation between the regular BH with ( $x = 2/3, c = 2$ ) and the Bardeen BH. Here, we have fixed  $l = 1$ .

Some similar phenomena have been observed in both cases. Without loss of generality, we fix  $l = 1$  and compare the QNMs with various  $n$ . Firstly, we notice that with the same deviation parameter  $\alpha_0$ , the discrepancy of the fundamental mode with  $n = 0$  is the minimal, while with the increase of  $n$ , the difference of the frequency becomes larger. Secondly, as the deviation parameter  $\alpha_0$  becomes larger, the overall discrepancy of the frequency becomes larger as well, implying that one could distinguish these two black holes easier. This tendency is understandable since the difference of the corresponding effective potential of these two black holes becomes more evident with the increase of  $\alpha_0$ .

## V. THE COMPARISON OF THE QNMS OF THIS SORT OF REGULAR BHS WITH DIFFERENT PARAMETERS X AND N

As we mentioned before, a sort of regular black holes with sub-Planck Kretschmann curvature can be constructed with the different choice of the parameter  $x$  and  $c$ , under the

$\alpha_0$	$n$	$\omega_{Regular}$	$\omega_{Bardeen}$	$\Delta$
0.15	0	0.254697-0.091332i	0.25479 - 0.091242 i	$7.4 \times 10^{-4} \%$
	1	0.223744-0.288622i	0.223744-0.288629i	0.0019%
	2	0.186622-0.513412i	0.186626-0.513428i	0.0030%
	3	0.159152-0.752567i	0.159167-0.752592i	0.0038%
	4	0.139809-0.995621i	0.139324-0.993985i	0.0047%
	5	0.125218-1.23947i	0.12527-1.239520i	0.0056%
0.58	0	0.276441-0.083850i	0.276483-0.084136i	0.10%
	1	0.250942-0.259415i	0.251826-0.260473i	0.38%
	2	0.210432-0.451302i	0.214505-0.452913i	0.88%
	3	0.158754-0.658531i	0.172191-0.656379i	2.00%
	4	0.111666-0.907950i	0.118232-0.866031i	4.64%
	5	0.089483-1.133720i	0.046411-1.131700i	3.79%

TABLE VII: A comparison of the QNMs under electromagnetic field perturbation between the regular BH with  $(x = 2/3, c = 2)$  and the Bardeen BH. Here, we have fixed  $l = 1$ .

condition  $c \geq x \geq c/3$  and  $c \geq 2$  [84]. Specially,  $(x = 2/3, c = 2)$  and  $(x = 1, c = 3)$  are just two typical regular black holes which have the identical asymptotic behavior at infinity as the famous Bardeen black hole and Hayward black hole, respectively. In this section, we intend to investigate the QNMs of this sort regular black holes and compare their behavior with different values of  $x$  and  $n$ .

We plot the trajectory of the QNMs on the plane of the frequency as the deviation parameter  $\alpha_0$  varies, where FIG. 12 is for  $l = 0, n = 0$  and FIG. 13 is for  $l = 0, n = 1$ .

Firstly, we look at FIG. 12 for the fundamental mode of the regular black holes with different  $x$  and  $c$ . In general, each trajectory starts from the same point which is identified as the frequency of Schwarzschild black hole, and exhibits the non-monotonic behavior with the similar shape. As  $\alpha_0$  runs from zero to the maximal value, the magnitude of the imaginary part is always smaller than the imaginary part of Schwarzschild black hole, no matter what values  $x$  and  $c$  are. Secondly, we notice that the trajectory moves toward the left as the parameter  $c$  increases, indicating that the non-monotonic behavior becomes pronounced. As a result, the maximal value of the real part of the frequency becomes smaller as  $c$  increases

and the real part with the maximal  $\alpha_0$ , which is the ending point of the trajectory, may be smaller than that of Schwarzschild black hole, as illustrated for  $c = 4$ . Thirdly, we notice that the trajectory of the regular black hole with  $(x = 2/3, c = 2)$  is overlapped with the trajectory of the regular black hole with  $(x = 1, c = 2)$ , implying it is independent of the parameter  $x$ . This results from the fact that in this setup we have set  $M = 1$ , thus the effect of  $x$  is absent. Nevertheless, we intend to argue that all the figures should be independent of the setup of Mass  $M$ , once one appropriately chooses the dimensionless quantity as the coordinate. For instance, taking  $\omega_R M$  and  $|\omega_I| M$  as the unit of the axes, then the figure should be independent of the setup of  $M$ .

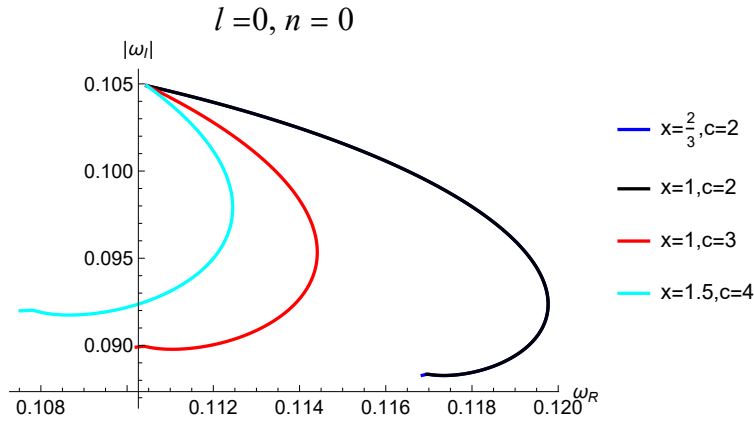


FIG. 12: The trajectory of the QNMs with the variation of  $\alpha_0$  on the frequency plane with  $l = 0$  and  $n = 0$  for regular black holes with various values of  $x$  and  $c$ .

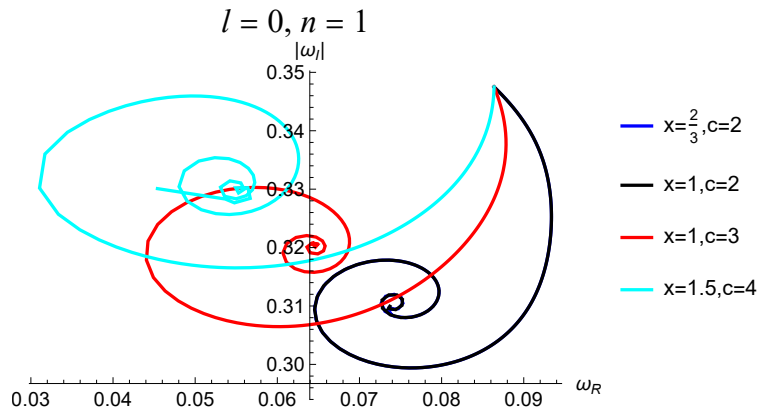


FIG. 13: The trajectory of the QNMs with the variation of  $\alpha_0$  on the frequency plane with  $l = 0$  and  $n = 1$  for regular black holes with various values of  $x$  and  $c$ .

Next we turn to FIG. 13 for ( $l = 0$  and  $n = 1$ ). In this case one notices that all the trajectories exhibit a spiral behavior, implying that the appearance of the spiral behavior of QNMs is only determined by the principal quantum number  $n$  and the angular quantum number  $l$ , irrespective of the parameter  $x$  and  $c$ . Secondly, for larger  $c$ , the real part of the QNMs decreases while the imaginary part increases such that the trajectory of the frequency moves to the left, indicating that the oscillation frequency of the QNM becomes weaker but the attenuation increases.

## VI. CONCLUSION AND DISCUSSION

In this paper we have computed the QNMs of a sort of regular black holes which is characterized by a Minkowskian core and sub-Planckian curvature with pseudo-spectral method and investigated the feature of these QNMs under the perturbations of scalar field and electromagnetic field, respectively. As a typical example, we have focused on the specific regular BH with fixed parameters  $x = 2/3$  and  $c = 2$ , which has the same asymptotic behavior at infinity with Bardeen black hole. It turns out that on the plane of the complex frequency, with the increase of  $n$ , the trajectory of the QNMs intends to exhibit a non-monotonic behavior, and then turn to a spiral behavior. For larger  $l$ , the value of  $n$  leading to spiral behavior becomes larger as well. At high overtones, the oscillation of the imaginary and real parts is referred to as the outburst of the overtone. We have also compared the QNMs of this regular black hole with those of the Bardeen BH. It is found that when the deviation parameter  $\alpha_0$  and the principal quantum number  $n$  are increased, the discrepancy between the QNMs of these two black holes becomes larger as well. Therefore, QNMs is undoubtedly a useful tool for distinguishing these BHs. Finally, we have compared the QNMs of the regular black holes with different  $x$  and  $c$ . We have found that the values of  $c$  and  $x$  do not change the non-monotonic and spiral behavior qualitatively, but with the increase of  $c$ , the real part of QNM decreases and the imaginary part increases overall, implying slower oscillations and stronger attenuation. Therefore, QNMs are also an effective tool to distinguish the regular BHs with different parameters  $x$  and  $c$ .

## Acknowledgments

We are very grateful to Zhong-wen Feng, Pan Li, Kai Li, Peng Liu, Wen-bin Pan, Meng-he Wu and Zhangping Yu for helpful discussions. Specially we would like to thank Wen-bin Pan, Meng-he Wu and Zhangping Yu for improving the code on the numerical simulation with PS method. This work is supported in part by the Natural Science Foundation of China under Grant No. 12035016 and 12275275. It is also supported by Beijing Natural Science Foundation under Grant No. 1222031, the Innovative Projects of Science and Technology No. E2545BU210 at IHEP, by Sichuan Youth Science and Technology Innovation Research Team with Grant No. 21CXTD0038, by and the National Natural Science Foundation of Sichuan Province with Grant No. 2023NSFSC1352, by The Central Guidance on Local Science and Technology Development Fund of Sichuan Province (2024ZYD0075), by the Sichuan Science and Technology Program (2023ZYD0023), and by Sichuan Science and Technology Program (2024NSFSC1999).

## Appendix A: Pseudo-spectral method

The pseudo-spectral method as a highly efficient numerical method is widely applied to solve various eigenvalue problems[100–105]. It also has an advantage in determining the QNMs of high overtones[48, 82, 106, 107]. The key in the pseudo-spectral method is to discretize the equation, and then transform the discretized equation into a generalized eigenvalue problem, solving for the eigenvalues. Usually, a continuous function is approximately represented by a sequence of its values on collocation points, which are usually selected as Chebyshev coordinates

$$x_i = \cos\left(\frac{i}{N}\pi\right), i = 0, \dots, N. \quad (\text{A1})$$

The second step is to construct the Chebyshev basis functions, which can be expressed as:

$$C_j(x) = \prod_{j=0, j \neq i}^N \frac{x - x_j}{x_i - x_j}. \quad (\text{A2})$$

Finally, the basis function is used to fit the objective function  $f(x)$ , which can be approximated as follows:

$$f(x) \approx \sum_{j=0}^N f(x_j)C_j(x). \quad (\text{A3})$$

The Chebyshev basis function can be expressed as:

$$C_j(x) = \frac{2}{Np_j} \sum_{m=0}^N \frac{1}{p_m} T_m(x_j) T_m(x), p_0 = p_N = 2, p_j = 1. \quad (\text{A4})$$

In the case of QNMs, due to the particularity of the boundary conditions, it is often convenient to use Eddington coordinates. We make the following substitution

$$r \rightarrow \frac{r_h}{u} \quad \text{and} \quad \Psi = e^{i\omega r_*(u)} \psi. \quad (\text{A5})$$

In this way, the coordinate  $u$  runs from 0 to 1. The wave equation in Eq.(12) under the scalar field perturbation transforms into the following expression:

$$\psi''(u) + \left[ \frac{f'(u)}{f(u)} + \frac{2ir_h\omega}{u^2 f(u)} \right] \psi'(u) - \left[ \frac{l(l+1)}{u^2 f(u)} + \frac{2ir_h\omega}{u^3 f(u)} \right] \psi(u) = 0. \quad (\text{A6})$$

While the wave equation for electromagnetic field perturbations transforms into the following expression:

$$\psi''(u) + \left[ \frac{f'(u)}{f(u)} + \frac{2ir_h\omega}{u^2 f(u)} \right] \psi'(u) - \left[ \frac{l(l+1)}{u^2 f(u)} + \frac{2ir_h\omega}{u^3 f(u)} + \frac{f'(u)}{u f(u)} \right] \psi(u) = 0. \quad (\text{A7})$$

Eq.(A6) and Eq.(A7) satisfy the boundary conditions at the horizon. In order to ensure that there are only outgoing waves at infinity, we take the following transformation for the variable:

$$\psi(u) = e^{\frac{2ir_h\omega}{u}} u^{2ir_h\omega f'(0)} \delta\psi(u), \quad (\text{A8})$$

then it can be checked that the boundary condition at infinity is automatically satisfied. Finally, we obtain the equation for scalar field perturbations and electromagnetic field perturbations, which satisfy the boundary conditions of having only incoming waves at the horizon and only outgoing waves at infinity. This equation is given by:

$$\delta\psi''(u) + \lambda_s(u)\delta\psi'(u) + \mu_s(u)\delta\psi(u) = 0. \quad (\text{A9})$$

Here,  $s = 0$  indicates scalar perturbation and  $s = 1$  indicates electromagnetic perturbation.  $\lambda_s$  and  $\mu_s$  have the following form:

$$\begin{aligned} \lambda_0(u) &= \frac{f'(u)}{f(u)} + \frac{4ir_h\omega f'(0)}{u} + \frac{2ir_h\omega}{u^2 f(u)} - \frac{4ir_h\omega}{u^2} \\ \mu_0(u) &= -\frac{l(l+1)}{u^2 f(u)} - \frac{2ir_h\omega[1+f(u)(-2+uf'(0))+uf'(u)(1-uf'(0))]}{u^3 f(u)} \\ &\quad - \frac{4r_h^2\omega^2(-1+uf'(0))[1+f(u)(-1+uf'(0))]}{u^4 f(u)}. \end{aligned} \quad (\text{A10})$$

$$\begin{aligned}
\lambda_1(u) &= \frac{4ir_h\omega f'(0)}{u} + \frac{f'(u)}{f(u)} + \frac{2ir_h\omega}{u^2 f(u)} - \frac{4ir_h\omega}{u^2} \\
\mu_1(u) &= \frac{8\omega^2 f'(0)r_h^2}{u^3} - \frac{4\omega^2 f'(0)r_h^2}{u^3 f(u)} - \frac{4\omega^2 f'(0)^2 r_h^2 + 2i\omega f'(0)r_h}{u^2} \\
&\quad - \frac{2i\omega r_h f'(u)}{u^2 f(u)} + \frac{2i\omega f'(0)r_h f'(u) - f'(u)}{u f(u)} + \frac{4\omega^2 r_h^2}{u^4 f(u)} - \frac{2i\omega r_h}{u^3 f(u)} \\
&\quad - \frac{l(l+1)}{u^2 f(u)} - \frac{4\omega^2 r_h^2}{u^4} + \frac{4i\omega r_h}{u^3}.
\end{aligned} \tag{A11}$$

Afterward, Eq.(A6) and Eq.(A7) transform into a generalized eigenvalue problem:

$$(M_0 + \omega M_1)\phi = 0. \tag{A12}$$

where  $M_i (i = 0, 1)$  are purely numerical matrices. Then, the frequency of QNMs can be obtained by solving the eigenvalues from Eq.(A12).

- 
- [1] H.-P. Nollert, *TOPICAL REVIEW: Quasinormal modes: the characteristic ‘sound’ of black holes and neutron stars*, *Class. Quant. Grav.* **16** (1999) R159–R216.
  - [2] K. D. Kokkotas and B. G. Schmidt, *Quasi-normal modes of stars and black holes*, *Living Reviews in Relativity* **2** (1999) 1–72.
  - [3] E. Berti, V. Cardoso, and A. O. Starinets, *Quasinormal modes of black holes and black branes*, *Classical and Quantum Gravity* **26** (2009), no. 16 163001.
  - [4] R. Konoplya and A. Zhidenko, *Quasinormal modes of black holes: From astrophysics to string theory*, *Reviews of Modern Physics* **83** (2011), no. 3 793–836.
  - [5] F. Echeverria, *Gravitational-wave measurements of the mass and angular momentum of a black hole*, *Physical Review D* **40** (1989), no. 10 3194.
  - [6] E. E. Flanagan and S. A. Hughes, *Measuring gravitational waves from binary black hole coalescences. ii. the waves’ information and its extraction, with and without templates*, *Physical Review D* **57** (1998), no. 8 4566.
  - [7] H. Yang, D. A. Nichols, F. Zhang, A. Zimmerman, Z. Zhang, and Y. Chen, *Quasinormal-mode spectrum of kerr black holes and its geometric interpretation*, *Physical Review D—Particles, Fields, Gravitation, and Cosmology* **86** (2012), no. 10 104006.
  - [8] G. T. Horowitz and V. E. Hubeny, *Quasinormal modes of ads black holes and the approach to thermal equilibrium*, *Physical Review D* **62** (2000), no. 2 024027.

- [9] R. A. Konoplya and A. Zhidenko, *Stability of multidimensional black holes: Complete numerical analysis*, *Nuclear Physics B* **777** (2007), no. 1-2 182–202.
- [10] R. A. Konoplya and A. Zhidenko, *Instability of higher-dimensional charged black holes in the de sitter world*, *Physical review letters* **103** (2009), no. 16 161101.
- [11] R. D. B. Fontana and F. C. Mena, *Quasinormal modes and stability of accelerating Reissner-Norsdröm AdS black holes*, *JHEP* **10** (2022) 047, [[arXiv:2203.13933](#)].
- [12] E. Berti, V. Cardoso, M. H.-Y. Cheung, F. Di Filippo, F. Duque, P. Martens, and S. Mukohyama, *Stability of the fundamental quasinormal mode in time-domain observations against small perturbations*, *Phys. Rev. D* **106** (2022), no. 8 084011, [[arXiv:2205.08547](#)].
- [13] K. Kyutoku, H. Motohashi, and T. Tanaka, *Quasinormal modes of Schwarzschild black holes on the real axis*, *Phys. Rev. D* **107** (2023), no. 4 044012, [[arXiv:2206.00671](#)].
- [14] S. Sarkar, M. Rahman, and S. Chakraborty, *Perturbing the perturbed: Stability of quasinormal modes in presence of a positive cosmological constant*, *Phys. Rev. D* **108** (2023), no. 10 104002, [[arXiv:2304.06829](#)].
- [15] R. D. B. Fontana, *Scalar field instabilities in charged BTZ black holes*, *Phys. Rev. D* **109** (2024), no. 4 044039, [[arXiv:2306.02504](#)].
- [16] D. Areán, D. G. Fariña, and K. Landsteiner, *Pseudospectra of holographic quasinormal modes*, *JHEP* **12** (2023) 187, [[arXiv:2307.08751](#)].
- [17] A. Courty, K. Destounis, and P. Pani, *Spectral instability of quasinormal modes and strong cosmic censorship*, *Phys. Rev. D* **108** (2023), no. 10 104027, [[arXiv:2307.11155](#)].
- [18] M. Skvortsova, *Quasinormal spectrum of  $(2+1)$   $(2+1)$ -dimensional asymptotically flat, ds and ads black holes*, *Fortschritte der Physik* **72** (2024), no. 6 2400036.
- [19] E. Berti, A. Sesana, E. Barausse, V. Cardoso, and K. Belczynski, *Spectroscopy of Kerr black holes with Earth- and space-based interferometers*, *Phys. Rev. Lett.* **117** (2016), no. 10 101102, [[arXiv:1605.09286](#)].
- [20] M. Giesler, M. Isi, M. A. Scheel, and S. Teukolsky, *Black Hole Ringdown: The Importance of Overtones*, *Phys. Rev. X* **9** (2019), no. 4 041060, [[arXiv:1903.08284](#)].
- [21] X. Jiménez Forteza, S. Bhagwat, P. Pani, and V. Ferrari, *Spectroscopy of binary black hole ringdown using overtones and angular modes*, *Phys. Rev. D* **102** (2020), no. 4 044053, [[arXiv:2005.03260](#)].
- [22] E. Maggio, L. Buoninfante, A. Mazumdar, and P. Pani, *How does a dark compact object*

- ringdown?*, *Phys. Rev. D* **102** (2020), no. 6 064053, [arXiv:2006.14628].
- [23] R. Dey, S. Biswas, and S. Chakraborty, *Ergoregion instability and echoes for braneworld black holes: Scalar, electromagnetic, and gravitational perturbations*, *Phys. Rev. D* **103** (2021), no. 8 084019, [arXiv:2010.07966].
- [24] G. Carullo, D. Laghi, N. K. Johnson-McDaniel, W. Del Pozzo, O. J. C. Dias, M. Godazgar, and J. E. Santos, *Constraints on Kerr-Newman black holes from merger-ringdown gravitational-wave observations*, *Phys. Rev. D* **105** (2022), no. 6 062009, [arXiv:2109.13961].
- [25] S. Yi, A. Kuntz, E. Barausse, E. Berti, M. H.-Y. Cheung, K. Kritos, and A. Maselli, *Nonlinear quasinormal mode detectability with next-generation gravitational wave detectors*, *Phys. Rev. D* **109** (2024), no. 12 124029, [arXiv:2403.09767].
- [26] R. F. Rosato, K. Destounis, and P. Pani, *Ringdown stability: greybody factors as stable gravitational-wave observables*, *arXiv preprint arXiv:2406.01692* (2024).
- [27] H. Nollert, *Characteristic oscillations of black holes and neutron stars: From mathematical background to astrophysical applications*, *unpublished Habilitationsschrift* (2000).
- [28] V. Ferrari and L. Gualtieri, *Quasi-Normal Modes and Gravitational Wave Astronomy*, *Gen. Rel. Grav.* **40** (2008) 945–970, [arXiv:0709.0657].
- [29] E. Berti, K. Yagi, H. Yang, and N. Yunes, *Extreme Gravity Tests with Gravitational Waves from Compact Binary Coalescences: (II) Ringdown*, *Gen. Rel. Grav.* **50** (2018), no. 5 49, [arXiv:1801.03587].
- [30] B. P. A. et al. (LIGO Scientific Collaboration and V. Collaboration), *Observation of gravitational waves from a binary black hole merger*, *Physical Review Letters* **116** (2016), no. 6 061102.
- [31] B. Abbott, R. Abbott, T. Abbott, S. Abraham, F. Acernese, K. Ackley, C. Adams, R. X. Adhikari, V. Adya, C. Affeldt, et al., *Tests of general relativity with the binary black hole signals from the ligo-virgo catalog gwtc-1*, *Physical Review D* **100** (2019), no. 10 104036.
- [32] D. Psaltis, L. Medeiros, P. Christian, F. Özel, K. Akiyama, A. Alberdi, W. Alef, K. Asada, R. Azulay, D. Ball, et al., *Gravitational test beyond the first post-newtonian order with the shadow of the m87 black hole*, *Physical review letters* **125** (2020), no. 14 141104.
- [33] E. Berti, V. Cardoso, and C. M. Will, *Gravitational-wave spectroscopy of massive black holes with the space interferometer lisa*, *Physical Review D—Particles, Fields, Gravitation,*

- and *Cosmology* **73** (2006), no. 6 064030.
- [34] K. Bronnikov, R. Konoplya, and A. Zhidenko, *Instabilities of wormholes and regular black holes supported by a phantom scalar field*, *Physical Review D—Particles, Fields, Gravitation, and Cosmology* **86** (2012), no. 2 024028.
- [35] A. Flachi and J. P. Lemos, *Quasinormal modes of regular black holes*, *Physical Review D—Particles, Fields, Gravitation, and Cosmology* **87** (2013), no. 2 024034.
- [36] Á. Rincón and V. Santos, *Greybody factor and quasinormal modes of regular black holes*, *The European Physical Journal C* **80** (2020) 1–7.
- [37] K. Jusufi, M. Azreg-Aïnou, M. Jamil, S.-W. Wei, Q. Wu, and A. Wang, *Quasinormal modes, quasiperiodic oscillations, and the shadow of rotating regular black holes in nonminimally coupled einstein-yang-mills theory*, *Physical Review D* **103** (2021), no. 2 024013.
- [38] C. Lan, Y.-G. Miao, and H. Yang, *Quasinormal modes and phase transitions of regular black holes*, *Nuclear Physics B* **971** (2021) 115539.
- [39] S. Hendi, S. Sajadi, and M. Khademi, *Physical properties of a regular rotating black hole: Thermodynamics, stability, and quasinormal modes*, *Physical Review D* **103** (2021), no. 6 064016.
- [40] R. Konoplya, Z. Stuchlik, A. Zhidenko, and A. Zinhailo, *Quasinormal modes of renormalization group improved dymnikova regular black holes*, *Physical Review D* **107** (2023), no. 10 104050.
- [41] K. Meng and S.-J. Zhang, *Gravito-electromagnetic perturbations and qnms of regular black holes*, *Classical and Quantum Gravity* **40** (2023), no. 19 195024.
- [42] L. López and V. Ramírez, *Quasi-normal modes of a generic-class of magnetically charged regular black hole: scalar and electromagnetic perturbations*, *The European Physical Journal Plus* **138** (2023), no. 2 120.
- [43] D. M. Gingrich, *Quasinormal modes of loop quantum black holes near the planck scale*, *Physical Review D* **109** (2024), no. 4 044044.
- [44] A. M. Simpson, *Ringing of the regular black hole with asymptotically minkowski core*, *Universe* **7** (2021), no. 11 418.
- [45] R. Konoplya and A. Zhidenko, *Infinite tower of higher-curvature corrections: Quasinormal modes and late-time behavior of d-dimensional regular black holes*, *Physical Review D* **109**

- (2024), no. 10 104005.
- [46] N. Franchini and S. H. Völkel, *Testing general relativity with black hole quasi-normal modes*, in *Recent Progress on Gravity Tests: Challenges and Future Perspectives*, pp. 361–416. Springer, 2024.
- [47] E. Franzin, S. Liberati, and V. Vellucci, *From regular black holes to horizonless objects: quasi-normal modes, instabilities and spectroscopy*, *Journal of Cosmology and Astroparticle Physics* **2024** (2024), no. 01 020.
- [48] D. Zhang, H. Gong, G. Fu, J.-P. Wu, and Q. Pan, *Quasinormal modes of a regular black hole with sub-planckian curvature*, *The European Physical Journal C* **84** (2024), no. 6 564.
- [49] J. Bardeen, *Non-singular general relativistic gravitational collapse*, in *Proceedings of the 5th International Conference on Gravitation and the Theory of Relativity*, p. 87, 1968.
- [50] I. Dymnikova, *Vacuum nonsingular black hole*, *General relativity and gravitation* **24** (1992) 235–242.
- [51] S. A. Hayward, *Formation and evaporation of nonsingular black holes*, *Physical review letters* **96** (2006), no. 3 031103.
- [52] V. P. Frolov, *Information loss problem and a ‘black hole’ model with a closed apparent horizon*, *Journal of High Energy Physics* **2014** (2014), no. 5 1–21.
- [53] R. Penrose, *Gravitational collapse and space-time singularities*, *Phys. Rev. Lett.* **14** (1965) 57–59.
- [54] S. W. Hawking and G. F. R. Ellis, *The Large Scale Structure of Space-Time*. Cambridge Monographs on Mathematical Physics. Cambridge University Press, 1973.
- [55] L. Xiang, Y. Ling, and Y. G. Shen, *Singularities and the Finale of Black Hole Evaporation*, *Int. J. Mod. Phys. D* **22** (2013) 1342016, [arXiv:1305.3851].
- [56] X. Li, Y. Ling, Y.-G. Shen, C.-Z. Liu, H.-S. He, and L.-F. Xu, *Generalized uncertainty principles, effective Newton constant and the regular black hole*, *Annals Phys.* **396** (2018) 334–350, [arXiv:1611.09016].
- [57] E. Bianchi, M. Christodoulou, F. D’Ambrosio, H. M. Haggard, and C. Rovelli, *White Holes as Remnants: A Surprising Scenario for the End of a Black Hole*, *Class. Quant. Grav.* **35** (2018), no. 22 225003, [arXiv:1802.04264].
- [58] A. Simpson and M. Visser, *Black-bounce to traversable wormhole*, *JCAP* **02** (2019) 042, [arXiv:1812.07114].

- [59] Z. Feng, Y. Ling, X. Wu, and Q. Jiang, *New black-to-white hole solutions with improved geometry and energy conditions*, *Sci. China Phys. Mech. Astron.* **67** (2024), no. 7 270412, [arXiv:2308.15689].
- [60] E. Ayon-Beato and A. Garcia, *Regular black hole in general relativity coupled to nonlinear electrodynamics*, *Physical review letters* **80** (1998), no. 23 5056.
- [61] L. Balart and E. C. Vagenas, *Regular black holes with a nonlinear electrodynamics source*, *Physical Review D* **90** (2014), no. 12 124045.
- [62] B. Koch and F. Saueressig, *Black holes within asymptotic safety*, *International Journal of Modern Physics A* **29** (2014), no. 08 1430011.
- [63] E. Ayón-Beato and A. Garcia, *The bardeen model as a nonlinear magnetic monopole*, *Physics Letters B* **493** (2000), no. 1-2 149–152.
- [64] Z.-Y. Fan and X. Wang, *Construction of regular black holes in general relativity*, *Physical Review D* **94** (2016), no. 12 124027.
- [65] A. Ashtekar, J. Olmedo, and P. Singh, *Quantum Transfiguration of Kruskal Black Holes*, *Phys. Rev. Lett.* **121** (2018), no. 24 241301, [arXiv:1806.00648].
- [66] A. Ashtekar, J. Olmedo, and P. Singh, *Quantum extension of the Kruskal spacetime*, *Phys. Rev. D* **98** (2018), no. 12 126003, [arXiv:1806.02406].
- [67] J. B. Achour, F. Lamy, H. Liu, and K. Noui, *Polymer schwarzschild black hole: An effective metric*, *Europhysics letters* **123** (2018), no. 2 20006.
- [68] Z.-W. Feng, Q.-Q. Jiang, Y. Ling, X.-N. Wu, and Z. Yu, *Symmetric black-to-white hole solutions with a cosmological constant*, arXiv:2408.01780.
- [69] A. Ashtekar, J. Olmedo, and P. Singh, *Regular black holes from loop quantum gravity*, in *Regular Black Holes: Towards a New Paradigm of Gravitational Collapse*, pp. 235–282. Springer, 2023.
- [70] C. Lan, H. Yang, Y. Guo, and Y.-G. Miao, *Regular black holes: A short topic review*, *International Journal of Theoretical Physics* **62** (2023), no. 9 202.
- [71] E. Berti and K. D. Kokkotas, *Asymptotic quasinormal modes of reissner-nordström and kerr black holes*, *Physical Review D* **68** (2003), no. 4 044027.
- [72] L.-G. Zhu, G. Fu, S. Li, D. Zhang, and J.-P. Wu, *Quasinormal modes of a charged loop quantum black hole*, arXiv preprint arXiv:2410.00543 (2024).
- [73] H. Gong, S. Li, D. Zhang, G. Fu, and J.-P. Wu, *Quasinormal modes of quantum-corrected*

- black holes*, *Phys. Rev. D* **110** (2024), no. 4 044040, [arXiv:2312.17639].
- [74] R. Konoplya, A. Zinhailo, J. Kunz, Z. Stuchlik, and A. Zhidenko, *Quasinormal ringing of regular black holes in asymptotically safe gravity: the importance of overtones*, *Journal of Cosmology and Astroparticle Physics* **2022** (2022), no. 10 091.
- [75] R. Konoplya, D. Ovchinnikov, and B. Ahmedov, *Bardeen spacetime as a quantum corrected schwarzschild black hole: Quasinormal modes and hawking radiation*, *Physical Review D* **108** (2023), no. 10 104054.
- [76] R. A. Konoplya, *Quasinormal modes and grey-body factors of regular black holes with a scalar hair from the Effective Field Theory*, *JCAP* **07** (2023) 001, [arXiv:2305.09187].
- [77] W.-L. Qian, G.-R. Li, R. G. Daghigh, S. Randow, and R.-H. Yue, *On universality of instability in the fundamental mode*, *arXiv preprint arXiv:2409.17026* (2024).
- [78] O. Stashko, *Quasinormal modes and gray-body factors of regular black holes in asymptotically safe gravity*, *Phys. Rev. D* **110** (2024), no. 8 084016, [arXiv:2407.07892].
- [79] D. M. Gingrich, *Quasinormal modes of a nonsingular spherically symmetric black hole effective model with holonomy corrections*, *Phys. Rev. D* **110** (2024), no. 8 084045, [arXiv:2404.04447].
- [80] R. Konoplya and A. Zhidenko, *Overtones' outburst of asymptotically ads black holes*, *Physical Review D* **109** (2024), no. 4 043014.
- [81] Z. S. Moreira, H. C. D. Lima Junior, L. C. B. Crispino, and C. A. R. Herdeiro, *Quasinormal modes of a holonomy corrected Schwarzschild black hole*, *Phys. Rev. D* **107** (2023), no. 10 104016, [arXiv:2302.14722].
- [82] G. Fu, D. Zhang, P. Liu, X.-M. Kuang, and J.-P. Wu, *Peculiar properties in quasinormal spectra from loop quantum gravity effect*, *Physical Review D* **109** (2024), no. 2 026010.
- [83] N. Franchini and S. H. Völkel, *Parametrized quasinormal mode framework for non-Schwarzschild metrics*, *Phys. Rev. D* **107** (2023), no. 12 124063, [arXiv:2210.14020].
- [84] Y. Ling and M.-H. Wu, *Regular black holes with sub-planckian curvature*, *Classical and Quantum Gravity* **40** (2023), no. 7 075009.
- [85] Y. Ling and M.-H. Wu, *Modified regular black holes with time delay and 1-loop quantum correction \**, *Chin. Phys. C* **46** (2022), no. 2 025102, [arXiv:2109.12938].
- [86] Y. Ling and M.-H. Wu, *The Shadows of Regular Black Holes with Asymptotic Minkowski Cores*, *Symmetry* **14** (2022), no. 11 2415, [arXiv:2205.08919].

- [87] A. Simpson, *Ringing of the Regular Black Hole with Asymptotically Minkowski Core*, *Universe* **7** (2021), no. 11 418, [[arXiv:2109.11878](#)].
- [88] W. Zeng, Y. Ling, Q.-Q. Jiang, and G.-P. Li, *Accretion disk for regular black holes with sub-planckian curvature*, *Physical Review D* **108** (2023), no. 10 104072.
- [89] W. Zeng, Y. Ling, and Q.-Q. Jiang, *Astrophysical observables for regular black holes with sub-planckian curvature*, *Chinese Physics C* **47** (2023), no. 8 085103.
- [90] E. W. Leaver, *An analytic representation for the quasi-normal modes of kerr black holes*, *Proceedings of the Royal Society of London. A. Mathematical and Physical Sciences* **402** (1985), no. 1823 285–298.
- [91] H. Cho, A. Cornell, J. Doukas, and W. Naylor, *Black hole quasinormal modes using the asymptotic iteration method*, *Classical and Quantum Gravity* **27** (2010), no. 15 155004.
- [92] K. Lin and W.-L. Qian, *The matrix method for black hole quasinormal modes*, *Chinese Physics C* **43** (2019), no. 3 035105.
- [93] K. Lin and W.-L. Qian, *A matrix method for quasinormal modes: Schwarzschild black holes in asymptotically flat and (anti-) de sitter spacetimes*, *Classical and Quantum Gravity* **34** (2017), no. 9 095004.
- [94] S. Fernando and J. Correa, *Quasinormal Modes of Bardeen Black Hole: Scalar Perturbations*, *Phys. Rev. D* **86** (2012) 064039, [[arXiv:1208.5442](#)].
- [95] B. Toshmatov, A. Abdujabbarov, Z. Stuchlík, and B. Ahmedov, *Quasinormal modes of test fields around regular black holes*, *Phys. Rev. D* **91** (2015), no. 8 083008, [[arXiv:1503.05737](#)].
- [96] M. Saleh, B. B. Thomas, and T. C. Kofane, *Quasinormal modes of gravitational perturbation around regular Bardeen black hole surrounded by quintessence*, *Eur. Phys. J. C* **78** (2018), no. 4 325.
- [97] K. Jusufi, M. Amir, M. S. Ali, and S. D. Maharaj, *Quasinormal modes, shadow and greybody factors of 5D electrically charged Bardeen black holes*, *Phys. Rev. D* **102** (2020), no. 6 064020, [[arXiv:2005.11080](#)].
- [98] Q. Sun, Q. Li, Y. Zhang, and Q.-Q. Li, *Quasinormal modes, Hawking radiation and absorption of the massless scalar field for Bardeen black hole surrounded by perfect fluid dark matter*, *Mod. Phys. Lett. A* **38** (2023), no. 22n23 2350102, [[arXiv:2302.10758](#)].
- [99] R. A. Konoplya, D. Ovchinnikov, and B. Ahmedov, *Bardeen spacetime as a quantum*

- corrected Schwarzschild black hole: Quasinormal modes and Hawking radiation*, *Phys. Rev. D* **108** (2023), no. 10 104054, [arXiv:2307.10801].
- [100] O. J. Dias, P. Figueras, R. Monteiro, J. E. Santos, and R. Emparan, *Instability and new phases of higher-dimensional rotating black holes*, *Physical Review D—Particles, Fields, Gravitation, and Cosmology* **80** (2009), no. 11 111701.
- [101] O. J. Dias, P. Figueras, R. Monteiro, H. S. Reall, and J. E. Santos, *An instability of higher-dimensional rotating black holes*, *Journal of High Energy Physics* **2010** (2010), no. 5 1–47.
- [102] K. Destounis, R. P. Macedo, E. Berti, V. Cardoso, and J. L. Jaramillo, *Pseudospectrum of reissner-nordström black holes: Quasinormal mode instability and universality*, *Physical Review D* **104** (2021), no. 8 084091.
- [103] J. L. Jaramillo, R. P. Macedo, and L. A. Sheikh, *Gravitational wave signatures of black hole quasinormal mode instability*, *Physical Review Letters* **128** (2022), no. 21 211102.
- [104] R. Monteiro, M. J. Perry, and J. E. Santos, *Semiclassical instabilities of kerr-anti-de sitter black holes*, *Physical Review D—Particles, Fields, Gravitation, and Cosmology* **81** (2010), no. 2 024001.
- [105] W. Xiong, P. Liu, C.-Y. Zhang, and C. Niu, *Quasinormal modes of the einstein-maxwell-aether black hole*, *Physical Review D* **106** (2022), no. 6 064057.
- [106] G. Fu, D. Zhang, P. Liu, X.-M. Kuang, Q. Pan, and J.-P. Wu, *Quasinormal modes and hawking radiation of a charged weyl black hole*, *Physical Review D* **107** (2023), no. 4 044049.
- [107] A. Jansen, *Overdamped modes in schwarzschild-de sitter and a mathematica package for the numerical computation of quasinormal modes*, *The European Physical Journal Plus* **132** (2017) 1–22.